

Document downloaded from:

<http://hdl.handle.net/10251/165954>

This paper must be cited as:

Tampau, A.; González Martínez, MC.; Vicente, AA.; Chiralt Boix, MA. (2020). Enhancement of PLA-PVA surface adhesion in bilayer assemblies by PLA aminolization. *Food and Bioprocess Technology*. 13(7):1215-1228. <https://doi.org/10.1007/s11947-020-02475-0>



The final publication is available at

<https://doi.org/10.1007/s11947-020-02475-0>

Copyright Springer-Verlag

Additional Information

1                   **Enhancement of PLA-PVA surface adhesion in bilayer assemblies**  
2                   **by PLA aminolization**

**Alina Tampau** <sup>a,1,\*</sup>, **Chelo González-Martínez** <sup>b,2</sup>, **António A. Vicente** <sup>c,3</sup>, **Amparo Chiralt** <sup>d,4</sup>

3           <sup>a, b, d</sup> Instituto Universitario de Ingeniería de Alimentos para el Desarrollo, Ciudad Politécnica de la Innovación,  
4                                   Universitat Politècnica de Valencia, Camino de Vera, s/n, 46022 Valencia, Spain.

5           <sup>c</sup> CEB – Centre of Biological Engineering, University of Minho, Campus de Gualtar, 4710-057 Braga, Portugal

6                                   <sup>1</sup> altam@upv.es, <sup>2</sup> cgonza@tal.upv.es, <sup>3</sup> avicente@deb.uminho.pt, <sup>4</sup> dchiralt@tal.upv.es

7  
8           **ABSTRACT**

9           Poly(lactic acid) (PLA) and poly(vinyl alcohol) (PVA) present complementary barrier  
10           properties and their combination in multilayer assemblies (laminates) could provide  
11           materials with more effective barrier capacity for food packaging purposes. However,  
12           their low chemical affinity compromises adequate polymer adhesion. Surface free  
13           energy modification of thermo-processed PLA films through treatment with 1,6-  
14           hexanediamine was used to enhance adhesion with polar PVA aqueous solutions.  
15           Treatments of 1 and 3 min increased the polar component of the solid surface tension,  
16           while treatments above 10 min provoked a corrosive effect in the films' structure.  
17           Extensibility analyses of PVA solutions loaded with carvacrol (15 wt. %) and different  
18           Tween 85 ratios on PLA activated surfaces allowed the selection of the 1 min  
19           aminolyzed surface for obtaining PLA-PVA bilayers, by casting PVA solutions on the  
20           PLA films. This study revealed that despite aminolization enhancing the PLA surface  
21           affinity for aqueous PVA solutions, casting-obtained bilayers presented limited oxygen  
22           barrier effectiveness due to heterogeneous thickness of PVA layer in the laminates.

23           **KEYWORDS:** aminolization; surface activation; poly(lactic acid); poly(vinyl alcohol);  
24           carvacrol; bilayer assembly.

25           **DECLARATIONS**

---

\* Corresponding author. E-mail address: altam@upv.es (Alina Tampau).

26 **Funding:** The authors acknowledge the financial support provided by the Ministerio de  
27 Economía y Competitividad (MINECO) of Spain (project AGL2016-76699-R). The  
28 author A. Tampau thanks MINECO for the pre-doctoral research grant #BES-2014-  
29 068100.

30 **Conflicts of interest/Competing interests:** The authors declare that they have no  
31 conflict of interest.

32 **Ethics approval:** Not applicable.

33 **Consent to participate:** Not applicable.

34 **Consent for publication:** Not applicable.

35 **Availability of data and material:** The raw/processed data required to reproduce these  
36 findings cannot be shared at this time due to legal or ethical reasons.

37 **Code availability:** Not applicable.

38 **Authors' contributions:** A. Tampau: *Writing - original draft, review & editing; Data*  
39 *curation; Investigation Methodology.* C. González-Martínez: *Supervision; Writing -*  
40 *review & editing.* A. A. Vicente: *Supervision; Writing - review & editing.* A. Chiralt:  
41 *Supervision; Writing - review & editing.*

42

## 43 1. Introduction

44 Biodegradable polymers have generated an increased interest in the current packaging  
45 field, as the massive use of conventional petroleum-based plastics has led to a negative  
46 environmental impact world-wide. Some biobased aliphatic polyesters, such as the  
47 polylactides, constitute a very promising group of materials for applications in the  
48 packaging area (Petersen et al., 1999). Poly(lactic acid) (PLA) is biocompatible (Food  
49 and Drug Administration approved) (Muller, González-Martínez, & Chiralt, 2017a),  
50 compostable (Farrington, Lunt, Davies, & Blackburn, 2005) and made from renewable  
51 sources. PLA presents potential as packaging material, as it can produce highly  
52 transparent, rigid films that exhibit low water vapour permeability (WVP) (Bonilla,  
53 Fortunati, Vargas, Chiralt, & Kenny, 2013; Collazo-Bigliardi, Ortega-Toro, & Chiralt,  
54 2018). Nevertheless, PLA also presents shortcomings, as it exhibits mechanical  
55 fragility/brittleness and limited oxygen barrier capacity (Bonilla et al., 2013).

56 A useful approach to offset drawbacks of individual films is by emulating the multilayer  
57 structure of commercial films. These are currently made of several sheets of polymers  
58 (3 to 12 layers according to <http://polymerdatabase.com/>) imparting complementary  
59 properties to the final material (e.g. European Patent EP0175451A2). Some layers  
60 provide moisture resistance, while others act as gas barriers or provide mechanical  
61 support, creating materials more suitable for the intended applications.

62 This strategy of pairing polymer sheets is already ongoing in the field of biopolymers.  
63 Several authors have reported obtaining multilayers with improved physical properties,  
64 based on starch and polyester combinations. Requena, Vargas, & Chiralt (2018)  
65 obtained bilayers by thermo-sealing cassava starch sheets, and polylactic acid-  
66 polyhydroxybutyrate-co-hydroxyvalerate blend films, with low WVP and good oxygen  
67 barrier capacity. Muller et al. (2017a) also obtained bilayer assemblies from thermo-  
68 processed cassava starch and amorphous PLA with improved barrier capacity with

69 respect to the corresponding monolayers. Rhim, Mohanty, Singh, & Ng, (2006)  
70 developed multilayer films based on a middle sheet of soy protein isolate (SPI) and  
71 exterior layers of polylactide obtained by casting. The tensile strength and barrier  
72 properties of the laminates also benefited from pairing the two polymers.

73 Poly(vinyl alcohol) (PVA) is a polar biopolymer with complementary barrier properties  
74 with respect to PLA, since its films possess a high barrier capacity to oxygen, with good  
75 tensile strength and flexibility (Cano et al, 2015). PVA has already been approved by  
76 the USDA to be used in the packaging of meat and poultry products. (DeMerlis &  
77 Schoneker, 2003). However, PVA exhibits high WVP due to its hydrophilic nature. Thus,  
78 the laminated assembly with hydrophobic polymer sheets, such as PLA, could yield a  
79 multilayer material with enhanced mechanical and barrier features.

80 One possible strategy to obtain multilayer films is the casting of a polymeric solution on  
81 the surface of another polymeric layer support. This method requires a good  
82 extensibility of the solution on the polymeric film, which is greatly affected by the surface  
83 interactions of the polymer solution with the supporting polymer that, in turn, depends  
84 on the molecular interactions between the components in the solution and those on the  
85 contact surface (Sapper & Chiralt, 2018). However, when using polymers with  
86 complementary properties, such as PVA and PLA, these are hydrophilic and  
87 hydrophobic in nature, respectively. Therefore, chemical affinity between them or their  
88 solutions is low, which compromises the surface interactions to obtain adequate  
89 polymer adhesion. To address this shortcoming, a potential strategy is the  
90 functionalization of the PLA surface through the aminolization technique. This method  
91 uses a diamine solution to introduce radicals carrying free amino moieties onto the  
92 surface of the PLA film (Zhu, Gao, Liu, & Shen, 2002). The ester (-COO-) groups in the  
93 polylactic acid chain would interact with one of the diamine's -NH<sub>2</sub> groups forming a  
94 covalent bond (O=C-NH-) (**Figure 1**). Thus, the diamine's structure carrying a free -NH<sub>2</sub>  
95 moiety would become attached to the polymer surface. The surface modifications in the

96 hydrophilic-lipophilic balance produced by the diamine can easily be monitored by  
97 observing the change in the surface energy components, through contact angle  
98 measurement. Then, the positively charged amino moieties (activated by immersion in a  
99 hydrochloric solution) could interact with a negatively charged polymer (such as partially  
100 acetylated PVA) in aqueous solution, generating a well-adhered coating on top of the  
101 PLA support material. This surface modification approach has found applications not  
102 only in constructing layer-by-layer assemblies for food coating application (Carneiro-da-  
103 Cunha et al., 2010; Pinheiro, Bourbon, Quintas, Coimbra, & Vicente, 2012; Medeiros,  
104 Pinheiro, Vicente, & Carneiro-da-Cunha, 2012; Medeiros et al., 2014; Fabra, Flores-  
105 López, Cerqueira, de Rodriguez, Lagaron, & Vicente, 2016), but also in live cell  
106 immobilization on the activated polyester surface (Zhu et al., 2002; Noel et al., 2013). In  
107 the previous studies for food packaging applications (Medeiros et al. 2012; Medeiros et  
108 al., 2014; Fabra et al. 2016; Souza et al. 2018) aminolysis functionalization technique  
109 was applied on a non-biodegradable polymer, polyethylene terephthalate (PET), to  
110 increase the adhesion of subsequently applied layers of polysaccharides or proteins  
111 containing active molecules. No previous aminolization studies on biodegradable  
112 polymeric supports to this end have been found.

113 The addition of antimicrobial or antioxidant molecules into the multilayer structure could  
114 provide additional benefits when used as packaging material, exerting an active  
115 protection on the packaged foodstuffs. Several studies have been carried out using  
116 different polymers and active compounds to obtain antimicrobial materials for food  
117 packaging. Anwar, Sugiarto and Warsiki (2018) reviewed previous studies, analyzing  
118 different incorporation methods (direct mixing, polishing, and encapsulation) of active  
119 compounds into the polymeric material in this packaging-making concept.

120 Carvacrol (CA) is a natural monoterpene present as a main constituent in the  
121 essential oils of oregano or thyme (Burt, 2004; Can Baser, 2008). It has proven  
122 antimicrobial and antioxidant effects, as reported by many authors (Kamimura, Santos,

123 Hill, & Gomes, 2014; Mascheroni, Guillard, Gastaldi, Gontard, & Chalier, 2011; Ramos,  
124 Beltrán, Peltzer, Valente, & Garrigós, 2014). The inclusion of CA in a carrier polymeric  
125 matrix could be a useful way to deliver its effects (Turek and Stintzing, 2013). In this  
126 sense, previous studies reported very slow release kinetics of these kinds of  
127 compounds from PLA films (Muller, Casado Quesada, González-Martínez, & Chiralt,  
128 2017b), whereas their encapsulation in more hydrophilic polymers (zein, chitosan,  
129 cassava and corn starch) favours the release, providing greater effectiveness as  
130 antimicrobial agents (Fabra et al., 2016; Muller et al., 2017b; Tampau, González-  
131 Martínez, & Chiralt, 2018).

132 Multilayer assemblies could incorporate the active compound into the polymer layer  
133 where the active compound is more effectively delivered in the target food to exert the  
134 antimicrobial or antioxidant action. The incorporation of the active compound in the  
135 polymer matrix modified barrier and mechanical properties of the film to a different  
136 extent, as reported by Requena et al. (2018) and Tampau et al. (2018) when carvacrol  
137 was incorporated into starch-polyester-blend bilayers and starch-PCL-starch  
138 multilayers, respectively.

139 Obtaining polyester sheets by the usual thermoprocessing and casting on their surface  
140 a film forming solution with a polar polymer ,such as PVA, with complementary barrier  
141 properties, is a feasible process to prepare laminates for food packaging purposes. The  
142 incorporation of the active compounds, such as carvacrol in the film forming solution,  
143 allows to avoid the thermal treatment of the active, preserving better its properties.

144 The aim of this study was to analyse the effect of the aminolization of thermo-processed  
145 PLA films on their surface energy (polar and dispersive components) and its impact on  
146 the extensibility of PVA aqueous solutions containing or not CA as active component,  
147 and surfactant. The functional properties of the bilayer assemblies as packaging  
148 material were also characterized to analyse the aminolization effect on the laminate  
149 properties.

## 150 **2. Materials and methods**

### 151 **2.1. Materials**

152 Poly(lactic acid) (PLA) 4060D (density 1.24 g/cm<sup>3</sup>; D-isomer content 12 % wt.) was  
153 acquired from Natureworks (Minnetonka, MN, USA) in the form of pellets. 1,6-diamino-  
154 hexane (for synthesis) was purchased from Merck Millipore Corporation (France), and  
155 2-propanol, hydrochloric acid and dimethyl sulfoxide from PanReac AppliChem  
156 (Castellar del Vallès, Barcelona, Spain). Ethyl acetate was acquired from Indukern (El  
157 Prat de Llobregat, Barcelona, Spain). Poly(vinyl alcohol) (PVA) (M<sub>w</sub> 13,000-23,000; 87-  
158 89% hydrolysed), polyoxyethylene sorbitan trioleate Tween 85 (S), carvacrol and  
159 phosphorous pentoxide (P<sub>2</sub>O<sub>5</sub>) were purchased from Sigma-Aldrich (Sigma-Aldrich  
160 Chemie, Steinheim, Germany). Ultrapure water (resistivity of 18.2 MΩ cm) was  
161 prepared using Milli Q Advantage A10 equipment from Millipore S.A.S., Molsheim,  
162 France.

### 163 **2.2. Mono- and bi- layer preparation**

#### 164 **PLA support monolayers**

165 Polylactic acid sheets were obtained by compression moulding. To this end, 4 g of the  
166 amorphous PLA pellets were placed on Teflon sheets in a hot plate press (Model LP20,  
167 Labtech Engineering, Thailand) and preheated for 4 min at 160 °C. Compression was  
168 applied for 4 min at 100 bar and 160 °C, followed by a cooling cycle of 3 min. The films  
169 thus obtained were kept in a desiccator with SiO<sub>2</sub> until used.

#### 170 **PLA /aminolization**

171 Surface aminolization of PLA was carried out as described by Zhu et al. (2004). Briefly,  
172 the PLA films were immersed in ethanol-water (1:1 v/v) solution for 2 h at room  
173 temperature to remove possible fatty residues adhered during manipulation. Afterwards,  
174 they were washed with abundant deionized water and dried in a vacuum oven at 30 °C  
175 for 24 h, until constant weight. The sheets were then immersed for different times (1, 3,



176 5, 10, 15 and 30 min) at 50 °C in 0.25 mol·L<sup>-1</sup> 1,6-hexanediamine solution in 2-propanol.  
177 A control sample immersed only in 2-propanol at 50 °C for the different times was also  
178 prepared. The treated surfaces were thoroughly rinsed with deionized water for 24 h at  
179 room temperature to remove traces of the unreacted diamine and dried in a vacuum  
180 oven (30 °C for 24 h). Similarly to Pinheiro et al. (2012) and Madeiros et al. (2012), the  
181 aminolized sheets were then immersed in a 0.1 mol·L<sup>-1</sup> hydrochloric acid solution for 3 h  
182 at room temperature, in order to positively charge the amino moieties grafted onto the  
183 surface. Then, the films were washed with abundant deionized water and dried again  
184 under vacuum at 30 °C for 24 h. The weight and thickness (measured by a Palmer  
185 digital micrometre from Comecta, Barcelona, Spain) of the dried materials were  
186 recorded. All the dried PLA films (treated and activated) were then stored in desiccators  
187 with SiO<sub>2</sub> until their use.

#### 188 **PVA /incorporation of actives**

189 PVA film-forming dispersions (FFDs) were prepared by dissolving the polymer (15 wt.  
190 %) in ultrapure water, under heating at 80 °C and constant magnetic stirring for one  
191 hour. Carvacrol (CA) was added at 15 wt. % with respect to the PVA content. These  
192 aqueous formulations were prepared with and without Tween 85 surfactant (S), using  
193 three different S:CA weight ratios: 0.3:100, 0.4:100 and 0.5:100. The first ratio value  
194 was considered based on an expected CA droplet diameter of 10 µm (Tampau,  
195 González-Martínez, & Chiralt, 2020) and a surfactant excess surface concentration of 5  
196 mg/m<sup>2</sup>, in the range of the previously reported values (Owusu Apenten & Zhu, 1996).  
197 This initial ratio was increased in order to determine possible benefits of an excess of  
198 surfactant on the wettability of PVA solutions. Afterwards, the dispersions were  
199 homogenized at 12,000 rpm for 3 min using an Ultra Turrax rotor–stator homogenizer  
200 (Model T25D, IKA Germany). CA-free FFD containing only PVA were also prepared as  
201 control. The FFDs were degassed under vacuum and allowed to rest at room  
202 temperature for 24 h to check their stability.

## 203 **Bilayer assembly**

204 The bilayer assemblies were obtained by coating the support PLA sheet (aminolized or  
205 not) with the selected PVA solutions. For this purpose, the aqueous solution, equivalent  
206 to 1.5 g of PVA polymer, was spread onto each PLA sheet by means of a manual spiral  
207 bar coater (100  $\mu\text{m}$ , Elcometer, UK). This implied a PVA/PLA wt. ratio of about 0.35 in  
208 the bilayer. The bilayers were allowed to dry at 21  $^{\circ}\text{C}$  and 55-60 % relative humidity  
209 (RH). Then, the dry materials were conditioned at 25  $^{\circ}\text{C}$  in desiccators with saturated  
210 solutions of  $\text{Mg}(\text{NO}_3)_2$  ensuring 53 % RH, until their characterization. The weights of the  
211 films were carefully recorded before and after the coating application to check the  
212 polymer wt. ratio. The prepared bilayers were labelled based on the untreated (PLA) or  
213 aminolized (am-PLA) support, and the applied PVA coating, carrying or not active (C)  
214 and/or surfactant (S) (e.g. am-PLA-PVA-C/S describes the bilayer obtained with PLA  
215 aminolized support and PVA layer containing both CA and S).

## 216 **2.3. Analyses of surface properties**

### 217 **Surface free energy of PLA films**

218 The surface free energy of the PLA sheets was assessed pre- and post-aminolization  
219 using the sessile drop method (Kwok & Neumann, 1999) by means of a contact angle  
220 meter (OCA 20 Dataphysics, Filderstadt, Germany). This involved measurement of the  
221 contact angle  $\theta$  between the analysed surface and different standard liquids of different  
222 polarities and known surface tensions. Dimethylsulfoxide (DMSO), ultrapure water, and  
223 ethyl acetate were used for this purpose. Their surface tension and dispersive and polar  
224 components are, respectively, 44.0, 36.0 and 8.0  $\text{mN}\cdot\text{m}^{-1}$  for DMSO, 72.8, 22.1 and  
225 50.7  $\text{mN}\cdot\text{m}^{-1}$  for water, and 23.9, 23.9 and 0.0  $\text{mN}\cdot\text{m}^{-1}$  for ethyl acetate  
226 ([www.accudynetest.com/surface\\_tension\\_table.html](http://www.accudynetest.com/surface_tension_table.html)). According to Hejda, Solař, &  
227 Kousal (2010), the surface free energy of the solid ( $\gamma_s$ ) can be expressed by Young's  
228 equation (**equation 1**):

$$229 \quad \gamma_S = \gamma_{SL} + \gamma_L \cdot \cos \theta \quad (1)$$

230 where:

231  $-\gamma_{SL}$  is interfacial tension solid-liquid;

232  $-\gamma_L$  is the surface tension of the liquid, and

233  $-\theta$  is the contact angle formed between the liquid-air interface and the solid surface.

234 If the polar and dispersive components acting at the interfacial tension are considered,

235 this surface interaction can be described by **equation 2**. Then, from the values of the

236 contact angle of pure solvents, with known dispersive ( $\gamma_L^d$ ) and polar ( $\gamma_L^p$ ) components,

237 on a determined surface, the plot of the variables according to equation 2 permits the

238 estimation of dispersive ( $\gamma_S^d$ ) (from the intercept of linear plot) and polar ( $\gamma_S^p$ ) (from the

239 slope of linear plot) components of the surface free energy (Sapper & Chiralt, 2018).

240 Solvent drops of 2  $\mu\text{L}$  were placed on the PLA surface and the contact angle was

241 determined at contact times of 0, 30 and 60 s. Ten replicates of the angle

242 measurements were carried out at room temperature ( $21 \pm 1$  °C) for each film sample

243 and solvent.

$$244 \quad \frac{1 + \cos \theta}{2} \cdot \frac{\gamma_L}{\sqrt{\gamma_L^d}} = \sqrt{\gamma_S^p} \cdot \sqrt{\frac{\gamma_L^p}{\gamma_L^d}} + \sqrt{\gamma_S^d} \quad (2)$$

## 245 **Surface tension of PVA solutions**

246 All PVA solutions were characterized in terms of their liquid-vapour surface tension ( $\gamma_{LV}$ )

247 using the same equipment as described for contact angle measurement. The surface

248 tension was estimated by applying the pendant drop method, using the Laplace-Young

249 approximation, as described by Ribeiro, Vicente, Teixeira, & Miranda (2007) and

250 Carneiro-da-Cuhna et al. (2009). Briefly, 10-12  $\mu\text{L}$  drops of the PVA solutions were

251 suspended at the flat end of a vertical needle and with the equipment's image

252 processing software the  $\gamma_{LV}$  was determined. At least thirty measurements at room  
253 temperature ( $21\pm 1$  °C) were taken for each solution.

#### 254 **Wettability of PVA solutions on PLA surface**

255 Wettability of the different PVA solutions (containing or not CA and S) was determined  
256 on the PLA film surface (aminolized or not). Wettability is assessed by calculating the  
257 spreading coefficient ( $W_s$ ) (**equation 3**) that represents the balance of the adhesion  
258 ( $W_a$ ) and cohesion ( $W_c$ ) works, as a function of the surface tension of the different PVA  
259 solutions and their contact angle on the PLA films (**equation 4**) (Sapper & Chiralt,  
260 2018). This parameter only yields a negative or zero value. The closer the value of  $W_s$  is  
261 to zero, the better that surface will be coated.

$$262 \quad W_s = W_a - W_c \quad (3)$$

$$263 \quad W_s = \gamma_L(\cos \theta - 1) \quad (4)$$

264 To this end, the measurement of the contact angle between PVA solutions and PLA  
265 films was taken, by using the sessile method described above. Ten measurements were  
266 carried out for each solution.

#### 267 **2.4. Surface microstructure**

268 The surface morphology of control and treated PLA was analysed by Field Emission  
269 Scanning Electron Microscopy (FESEM Ultra 55, Zeiss, Oxford Instruments, UK). For  
270 this purpose, the surface of monolayers was observed without any additional treatment,  
271 whereas bilayers were previously cryo-fractured by immersion in liquid nitrogen to allow  
272 for cross-section view. Samples were mounted with carbon tape on stubs, and after  
273 sputtering with platinum in an EM MED020 (Leica Microsystems, Germany), were  
274 observed under an accelerating voltage of 1 kV.

#### 275 **2.5. Analysis of functional properties of bilayer films**

## 276 **Water vapour and oxygen permeability**

277 Water vapour permeability (**WVP**) of bilayers was assessed at 25 °C and 53-100 % RH  
278 gradient, using ASTM E96-95 gravimetric method (ASTM, 1995), and considering the  
279 modification proposed by Gennadios, Weller, & Gooding (1994). Briefly, previously  
280 conditioned samples were fitted onto Payne aluminium cups (diameter of 3.5 cm)  
281 (Elcometer SPRL, Hermelle/s Argenteau, Belgium) containing 5 mL of deionized water  
282 and were placed in desiccators with saturated  $\text{Mg}(\text{NO}_3)_2$  aqueous solution. A small fan  
283 was placed on top of each cup to favour the water vapour transport. The cups were  
284 weighed periodically with an analytical balance ( $\pm 0.00001$  g) and weight loss vs. time  
285 was plotted to obtain the water vapour transmission rate (WVTR). Then, the WVP was  
286 calculated as described by Perdones, Chiralt, & Vargas (2016). Measurements were  
287 carried out in triplicate.

288 The oxygen permeability (**OP**) of conditioned samples was determined at 25 °C and  
289 53 % RH, following the guidance of Standard Method D3985-05 (ASTM, 2005). The  
290 equipment OXTRAN (Mocon Lippke, Neuwied, Germany) was used to determine the  
291 oxygen transmission rate (OTR). Film samples (area of 50 cm<sup>2</sup>) were exposed to pure  
292 oxygen flow on one side and pure nitrogen flow on the opposite side. The oxygen  
293 transmission values were registered every 10 min until equilibrium was reached. Then  
294 the OP was determined as described by Cano, Jiménez, Cháfer, González, & Chiralt  
295 (2014), taking into account the samples' thickness. At least two replicates per  
296 formulation were considered.

## 297 **Mechanical properties**

298 The tensile properties of the materials were assessed with a universal test machine  
299 (TA.XT plus model, Stable Micro Systems, Haslemere, England) following the  
300 guidelines of ASTM standard method D882 (ASTM, 2001), as previously described by  
301 Ortega-Toro, Contreras, Talens, & Chiralt (2015). Conditioned samples (25x100 mm)

302 were fixed in the machine's extension grips (positioned 50 mm apart) and stretched at  
303 50 mm·min<sup>-1</sup> until break. Tensile strength at break (TS), Young modulus (YM) and  
304 elongation at break ( $\epsilon\%$ ) were obtained from the stress-strain curves. A minimum of  
305 eight measurements per sample were taken.

## 306 **Optical properties**

307 The samples were analysed in terms of their transparency, by means of internal  
308 transmittance ( $T_i$ ) assessed by applying the Kubelka-Munk theory for multiple scattering  
309 (Hutchings, 1999), as previously reported by Ortega-Toro et al. (2015). A  
310 spectrophotometer CM-3600d (Minolta Co., Tokyo, Japan) was used to determine the  
311 surface reflectance spectra (wavelength range 400-700 nm) against black and white  
312 backgrounds. The value of  $T_i$  at 460 nm was selected as the benchmark value for  
313 sample comparison.

## 314 **2.6. Thermogravimetric analysis (TGA) and differential scanning calorimetry** 315 **(DSC)**

316 Previously P<sub>2</sub>O<sub>5</sub> conditioned films were submitted to thermal analyses. Their thermal  
317 degradation (TGA) was analysed with a thermo-gravimetric analyser (TGA/SDTA 851e,  
318 Mettler Toledo, Schwarzenbach, Switzerland). To this end, approximately 10 mg of  
319 samples were placed into alumina crucibles (capacity 70  $\mu$ L) and heated from 25 to  
320 600 °C at a rate of 10 K/min, under nitrogen flow (20 mL/min). The thermal weight loss  
321 curves (TA) and their derivatives (DTA) were obtained and the onset, peak and endset  
322 temperatures for each degradation peak were extracted by using the STARe Evaluation  
323 Software (Mettler-Toledo, Inc., Switzerland). For the DSC analyses, a triple step thermal  
324 scan was applied using DSC equipment (1 StarE System, Mettler-Toledo, Inc.,  
325 Switzerland). Samples were cooled and kept at -25 °C for 5 min and then heated at  
326 10 K/min from -25 to 200 °C, where they were maintained for 2 min. Then, samples

327 were cooled from 200 to -25 °C at 10 K/min, maintained at -25 °C for 5 min and  
328 afterwards heated from -25 to 250 °C, at 10 K/min. As reference, an empty aluminium  
329 pan was used. All thermal analyses were done in duplicate.

## 330 **2.7. Statistical analysis**

331 The analysis of the data was performed through variance analysis (ANOVA) using the  
332 Statgraphics Centurion XVII.64 software (Statgraphics Technologies, Inc., Warrenton,  
333 VA, USA). The Fisher Least Significant Difference (LSD) was used to evaluate the  
334 differences ( $p < 0.05$ ) among the samples' means.

## 335 **3. Results and Discussion**

### 336 **3.1. Changes in the PLA surface induced by aminolization**

337 The aminolization process of the PLA surface was followed through the changes in the  
338 surface energy (SE) of the films (polar and dispersive components) and microstructural  
339 observations of the film surface by FESEM. Contact angles of the different solvents on  
340 the PLA surface were constant with time for all pure solvents, except for ethyl acetate  
341 where changes occurred mainly due to the solvent volatility. Thus, only the contact  
342 angle value for 0 seconds contact time were considered. From the contact angle  
343 measurements, and taking into account the values of the dispersive and polar  
344 components of the surface tension for the different pure solvents, the values of  
345 dispersive and polar components of the surface energy of PLA films were obtained. To  
346 this end, the linear fitting of eq. 2, according to the variable combinations shown in the  
347 equation, was carried out. These obtained values are shown in **Table 1** for the surfaces  
348 aminolized for different times. The total surface energy (sum of both components) was  
349 also determined at each aminolization time. A notable increase (of almost 100 %) in the  
350 polar component value was observed at the shortest treatment times (1 and 3 min). The  
351 film submitted to the 5 min treatment did not show a similar trend, having values of the

352 SE components that were more similar to the untreated sample. The changes (%  
353 relative to the initial value) in mass and thickness of treated samples are also shown in  
354 **Table 1**. Both parameters increased with treatment time, probably due to solvent  
355 adsorption and retention in the polymer matrix and its subsequent swelling. In fact,  
356 samples immersed only in solvent at the same temperature also gained mass, but in a  
357 lower proportion, as shown in **Table 1** (values in brackets). In control treatments using  
358 only solvent, the mass gain was greater than in the reactive samples for all treatment  
359 times and reached a constant value of about 8 % from 5 min immersion onwards. This  
360 indicates that in the presence of reactive, mass change also involves other mechanisms  
361 related with the reaction, which could imply losses through the polymer solubilisation in  
362 the reactant media. In fact, the sample treated for 30 min exhibited a net weight loss,  
363 while the film thickness greatly increased, thus revealing the effective mass loss of the  
364 highly swollen film due to its partial solubilisation in the solvent-reactive system. Then, a  
365 prolonged contact with the diamine leads to a high degree of erosion/dissolution of the  
366 polylactide. Additionally, beyond the 10 min mark, the post-aminolization samples were  
367 visibly brittle. So, they were considered physically unfit for use in the subsequent  
368 coating step, as they would provide little mechanical support for the bilayers.

369 The FESEM micrographs in **Figure 2** show the surface aspect of the PLA films where  
370 the changes provoked by the aminolization process at different times can be observed.  
371 The initial relatively rough surface of the untreated polylactide films shows a gradual  
372 smoothing at short aminolization times (1 and 3 min), as also observed by other  
373 authors (Drobot et al. 2013). This can be attributed to the solubilisation of the more  
374 emerging zones of the rough surface overlapping with the aminolization of the surface  
375 chains, as revealed by the increase in the polar component of the film surface energy.  
376 However, a more irregular surface was observed at 5 min treatments where the surface  
377 tension polar component decreased. This suggests that aminolized chains could  
378 prevalently solubilise during treatment, generating an irregular film surface. For the 10



379 min treatment, visible voids can be observed in the films, confirming the internal action  
380 of the 1,6-hexane diamine reactive and partial solubilisation of the film material. The  
381 internal diffusion of the reactive and solvent into the films seems to produce a highly  
382 porous structure at 15 and 30 min treatments, as revealed by the visible pores in the  
383 film microstructure and the great increase in the film thickness. At the end of the latter  
384 treatment, the intense erosion of the films structure can be clearly observed in **Figure 2**,  
385 where a high ratio of voids and pores can be seen on the film surface, while the films  
386 appeared highly deformed after drying. In fact, the measurements of contact angle were  
387 not possible in these distorted films. Film immersion in pure solvent did not provoke a  
388 great alteration in the film surface beyond the leaching of the most superficial chains  
389 that changed the surface aspect of the films compared with the initial samples (**Figure**  
390 **2**).

391 The obtained results indicate that aminolization of PLA films must be carried out for  
392 short times (1 or 3 min) where the polar component of the film surface tension  
393 increased. Longer treatment times provoked internal damage in the film structure  
394 associated with the internal diffusion of reactants and solvent that provoked the swelling  
395 of the polymer matrix and the partial solubilisation of the film components.

#### 396 **Wettability of PLA with PVA liquid systems**

397 PLA films treated at 0, 1 and 3 min aminolization (when the polar component of surface  
398 energy increased) were submitted to the wettability test with the PVA  
399 solutions/emulsions prepared as described in section 2.2, containing or not carvacrol  
400 and different ratios of surfactant. Contact angles obtained between PVA liquid systems  
401 and the PLA films treated for different times are shown in **Table 2**, as well as the values  
402 of surface tension of the different PVA liquid systems. All contact angles were below  
403 90°, indicating that the surface can be wetted by the liquids. The surface tension ( $\gamma_L$ ) of  
404 the PVA liquid systems was significantly reduced by carvacrol incorporation, whereas  
405 no significant effect of the surfactant was observed at any ratio. The effect of the

406 emulsified carvacrol on the surface tension of PVA solution can be attributed to the  
407 presence of small droplets of the compound at the liquid surface that modify the  
408 interfacial interaction forces due to its more hydrophobic nature. Likewise, the lack of a  
409 significant surfactant effect on the surface tension of the carvacrol emulsions could be  
410 due to its prevalent location at the oil-water interface and the main effect of carvacrol  
411 droplets at the surface level. This behaviour was also observed by Sapper, Bonet and  
412 Chiralt (2019) when thyme essential oil was emulsified in an aqueous solution of  
413 cassava starch-gellan with and without surfactant.

414 As concerns the contact angle, it decreased (from 51 to 33) for pure PVA solutions as  
415 the polar component of surface tension increased during aminolization, thus reflecting  
416 the greater chemical affinity between the aminolized PLA surface and PVA aqueous  
417 solutions. However, for the PVA solution with emulsified carvacrol, the contact angle of  
418 non-aminolized PLA was lower (44) and less sensitive to the aminolization time. This  
419 agrees with the greater surface affinity of the carvacrol-containing liquid with the initial  
420 PLA surface. In fact, the contact angle of this emulsion increased in the case of the 3  
421 min aminolization treatment. The presence of surfactant provoked small changes in the  
422 contact angle, which could be attributed to specific interactions of the amphiphilic  
423 molecule with the PLA surface that affect the global surface forces at the solid-liquid-air  
424 contact. The small ratio of surfactant was more effective at decreasing the contact angle  
425 in non-aminolized PLA surfaces than the higher proportions, whereas it was not  
426 effective at reducing the contact angle in aminolized PLA surfaces.

427 The wettability parameter ( $W_s$ ) values calculated for the different PVA formulations and  
428 PLA surfaces are also shown in **Table 2**. The further from zero the values of  $W_s$  are, the  
429 less likely it is for that formulation to spread well over the PLA surface. Therefore, the  
430 best extensibility was obtained for 3 min treated PLA films with pure PVA solutions, for 1  
431 min treated PLA films with PVA solution with emulsified carvacrol and for 0 min treated  
432 PLA support when emulsions contained the lowest ratio of surfactant. Therefore, 1 min

433 aminolized PLA support could be a compromise point to achieve a good extensibility of  
434 the different PVA liquid systems while the lowest ratio of surfactant was more adequate  
435 to enhance the liquid phase extension. This choice implies an improvement in the  
436 extensibility of the pure PVA solution on PLA films, while a similar extensibility of the  
437 three PVA formulations (without and with carvacrol, containing or not surfactant) would  
438 be achieved. Thus, from this study, the aminolization time selected for the subsequent  
439 application was 1 min, and the PLA films treated for 1 min were coated with PVA,  
440 PVA/C and PVA/C-S (0.3:100) formulations to obtain bilayer films whose functional  
441 properties were characterized.

### 442 **3.2. Functional properties of PLA-PVA bilayer films**

443 The obtained bilayer films exhibited a thickness of 230-250  $\mu\text{m}$  from which  
444 approximately 22 % corresponded to the PVA layer ( $56\pm 21$   $\mu\text{m}$  average value) and the  
445 rest to the PLA sheet ( $195\pm 11$   $\mu\text{m}$  average value). These values are coherent with the  
446 mass ratio of each polymer in the laminate (approximately 0.27 for PVA). However, at  
447 microscopic level a higher heterogeneity in the PVA thickness was detected, depending  
448 on the film sample. **Figure 3** shows FESEM micrographs of some bilayer films where  
449 differences in the overall thickness of the PVA sheet can be seen, as well as differences  
450 in the thickness along a determined film, depending on the roughness of the PLA  
451 surface.

452 When a small protuberance appeared in the PLA surface (dotted arrows, **Figure 3**), the  
453 PVA layer was thinner, which can be critical when the coating was very thin. This aspect  
454 could compromise the barrier capacity provided by the PVA layer in the zones where its  
455 thickness was extremely thin (about 10  $\mu\text{m}$ ). Then, in the laminates obtained by casting  
456 PVA solutions on PLA surface, the more hydrophobic PLA layer was thicker, whereas  
457 the cast hydrophilic layer of PVA was thinner with great variability in thickness, which

458 could influence its effectiveness at controlling its barrier capacity (Debeaufort, Martin-  
459 Polo, & Voilley, 1993).

460 Given that most deteriorative processes in foods are caused by water or oxygen  
461 exchanges, food packaging materials require a good barrier capacity against moisture  
462 and oxygen to extend foodstuff shelf life (Cerqueira, Lima, Teixeira, Moreira, & Vicente,  
463 2009). The WVP and OP of the obtained bilayers are shown in **Table 3**, together with  
464 the corresponding values of each monolayer. According to the Ideal Laminate Theory  
465 (Siracusa, 2012), the polymer layer with lower permeability usually determines the  
466 barrier capacity of laminates for water vapour or gases. As such, the WVP values of  
467 bilayers were expected to be around those of the PLA sheet that exhibited the lowest  
468 WVP. Indeed, the WVP of bilayers present similar values to those of the PLA monolayer  
469 with small differences between the different samples. Laminates with aminolized PLA  
470 exhibited a wider WVP range, the bilayer with the pure PVA sheet being the one with  
471 the lowest value.

472 However, the values of oxygen permeability were not in the range of that of the PVA  
473 sheet that should be the limiting layer for oxygen transmission. Both the aminolized  
474 bilayers and those non-aminolized with pure PVA showed similar OP values to those of  
475 the PLA monolayer. In contrast, non-aminolized laminates containing carvacrol (with  
476 and without surfactant) exhibited lower OP values. This could be attributed to the  
477 oxygen-blocking effect exerted by the antioxidant CA, but this was not observed in  
478 bilayers with aminolized PLA. The lack of effectiveness of PVA sheets in reducing the  
479 OP of laminates could be due to the heterogeneous coating at microscopic level that  
480 should generate regions in the films with very thin hydrophilic coating. Thus, oxygen  
481 transfer would take place, mainly limited by the PLA sheet.

482 The tensile properties (Young modulus (YM), tensile strength (TS) and elongation ( $\epsilon$ ) at  
483 break) of bilayers are also presented in **Table 3**. The bilayers exhibited tensile property  
484 values in the range of the stiffest PLA sheet, which also represents the thickest layer of

485 the assembly. The films containing CA with and without surfactant had the lowest  
486 values of YM, regardless of the aminolization of the PLA sheet. This could be explained  
487 by the partial carvacrol migration into the PLA sheet, weakening the inter-chain forces of  
488 the PLA matrix. This effect was also appreciated in the values of the bilayer's resistance  
489 to break (TS), which were higher when neither CA nor T85 were present, showing  
490 values similar to those of the PLA monolayer. All materials had elongation at break  
491 values of under 10 %, denoting a quite brittle behaviour, in the order of PLA films.  
492 However, a slight increase in the film extensibility could be appreciated for the CA-  
493 carrying laminates, in line with the plasticising effect of the CA that potentially migrated  
494 into the PLA sheets.

495 The internal transmittance ( $T_i$ ), also presented in **Table 3**, is directly related to the film  
496 transparency. All of the aminolized sheets presented a cloudiness (photos not shown)  
497 as result of the aminolization step. This explains the decrease in the  $T_i$  parameter for  
498 these treated materials. However, this acquired opacity could be considered positive for  
499 certain food packaging applications where a reduction in light-induced oxidative  
500 reactions is required.

501 The results indicate that bilayer PLA-PVA films obtained by casting PVA aqueous  
502 solutions onto the PLA surface did not provide additional benefits to the PLA  
503 monolayers. The expected, the barrier capacity against oxygen potentially imparted by  
504 the PVA sheet was not effective, while the PVA did not contribute to the mechanical  
505 reinforcement of the PLA layer. Despite PLA aminolization enhancing the polar nature  
506 of the PLA surface and thus the chemical affinity with the PVA aqueous solutions to be  
507 extended, the obtained PVA coatings were heterogeneous in thickness and the thinner  
508 regions seem to limit the barrier capacity of the coating against oxygen.

### 509 **3.3. Thermal behaviour as affected by the aminolization treatment**

510 A thermal analysis of the obtained materials was carried out in order to discover the  
511 effect of aminolization and lamination on the physical state of polymers, which, in turn,  
512 affects their functional properties. **Table 4** summarizes the degradation temperatures of  
513 the different samples, as obtained by thermogravimetric analysis. TGA thermographs  
514 (**Figure 4**) show an overlapping of the degradation steps of both polymers due to due to  
515 the proximity of its degradation temperature range. The aminolization process did not  
516 modify the degradation temperature of PLA, the peak being at 310 °C. PVA starts its  
517 degradation and exhibits the peak at a lower temperature (192/288 °C) than the PLA.  
518 Thus, bilayers showed notable  $T_{\text{onset}}$  values in the range of 240-255 °C, lower than that  
519 of pure PLA (269 °C). A second and third small degradation peak appeared in bilayers  
520 at about 390 and 500 °C, which could be attributed to the PVA degradation in  
521 subsequent steps as described by other authors (Bonilla et al., 2014; Cano et al., 2016).  
522 No significant differences were observed between the degradation behaviour of the  
523 different bilayers. No thermo-release of carvacrol from the corresponding bilayers was  
524 detected, probably due to the very small mass fraction of the compound in the laminate:  
525 about 11 g/g PVA, according to previous studies (Tampau et al., 2020). **Table 4** also  
526 shows the glass transition temperature ( $T_g$ ) for the different materials obtained in the  
527 first and second heating scans. In the first heating step, two distinct  $T_g$  can be observed,  
528 corresponding to the two polymers present in bilayers. For samples without carvacrol,  
529 the first one, at a slightly lower temperature, corresponds to the PLA, while the second  
530 one must be attributed to the PVA. For laminates without carvacrol, both transitions  
531 practically overlap, but these are more decoupled for bilayers with carvacrol due to the  
532 plasticizing effect of the compound that shifts the transition of the PVA sheet to a lower  
533 temperature, below the  $T_g$  of PLA. The DSC thermograms (**Figure 5**) also revealed the  
534 typical relaxation of PLA after  $T_g$  in the first heating step, associated with polymer  
535 ageing (Muller, Jiménez, González-Martínez, & Chiralt, 2016). However, as the thermal  
536 history of the materials is erased and they become melt blended in the first step, only a

537 single  $T_g$  was observed in the second heating, without relaxation enthalpy. This  $T_g$  value  
538 was lower for laminates with carvacrol, thus indicating the plasticizing effect of the  
539 compound on the melt blended polymer matrix.

540 Likewise, PVA crystallizes in the laminate and the melting temperature and enthalpies  
541 are shown in **Table 4**. Polymer melting was observed from about 160 °C, with a peak at  
542 about 185°C, in agreement with other studies (Tampau et al., 2020). However, a high  
543 degree of variability was observed in the melting enthalpy of PVA when expressed per g  
544 of polymer, in both the first and second (values not shown) heating steps, assuming a  
545 constant mass fraction of PVA in the bilayer film. Nevertheless, the variable thickness  
546 observed in the layers could imply notable differences in the PVA ratio in the DSC  
547 analysed samples. This could explain the variability in the melting enthalpy and  
548 corroborate the heterogeneous coating in the bilayer obtained by casting.

549 Therefore, DSC analyses revealed the amorphous state of PLA and the semicrystalline  
550 nature of PVA in the laminates, without any appreciable effect of the PLA aminolization.  
551 However, the variability in the PVA melting enthalpy points to the heterogeneity of the  
552 coating on the laminate obtained by casting, even in the case of aminolized PLA, where  
553 wettability was enhanced.

#### 554 **4. Conclusions**

555 The aminolization technique applied for less than 3 min yields PLA surfaces with a  
556 greater polar component of the surface free energy (100% increase), thus enhancing  
557 wettability with polar solutions of PVA. The prolonged (>3 min) exposure to 1,6-  
558 hexanediamine had negative effects on the polar component and microstructure of the  
559 PLA films. Extensibility of the liquid phase containing carvacrol on the PLA sheet was  
560 not improved by aminolization. Mechanical and barrier properties of PLA-PVA bilayers  
561 containing, or not, carvacrol were not significantly affected by the aminolization  
562 treatment and were very close to the properties of the major PLA monolayer. Therefore,

563 the PVA sheet did not provide the expected oxygen barrier capacity to the laminate.  
564 Carvacrol promoted the bilayer stretchability due to its plasticising effect on both PVA  
565 and PLA sheets. Thus, coating PLA sheets (aminolized or not) with PVA solutions is not  
566 recommended for the purposes of obtaining laminates for food packaging applications,  
567 since neither the barrier nor the mechanical properties were an improvement on those  
568 of PLA films, mainly due to the heterogeneous thickness of the PVA coating.

569 **Funding:** The authors acknowledge the financial support provided by the Ministerio de  
570 Economía y Competitividad (MINECO) of Spain (project AGL2016-76699-R). The  
571 author A. Tampau thanks MINECO for the pre-doctoral research grant #BES-2014-  
572 068100.

573 **Conflict of Interest:** The authors declare that they have no conflict of interest.

## 574 **5. References**

575 ASTM. (1995). Standard test methods for Water Vapor Transmission of materials.  
576 Standard designations: E96-95. Annual book of ASTM standards, Philadelphia,  
577 PA: American Society for Testing and Materials (pp. 406–413).

578 ASTM. (2001). Standard test method for tensile properties of thin plastic sheeting.  
579 Standard D882. Annual book of American standard testing methods. Philadelphia,  
580 PA: American Society for Testing and Materials (pp. 162–170).

581 ASTM. (2005). Standard test method for oxygen gas transmission rate through plastic  
582 film and sheeting using a coulometric sensor. Standard designations: 3985-05.  
583 Annual book of ASTM standards. West Conshohocken, PA: American Society for  
584 Testing and Materials.

585 Bonilla, J., Fortunati, E., Vargas, M., Chiralt, A., & Kenny, J. M. (2013). Effects of  
586 chitosan on the physicochemical and antimicrobial properties of PLA films. *Journal*  
587 *of Food Engineering*, 119(2), 236–243.



588 Bonilla, J., Fortunati, E., Atarés, L., Chiralt, A., & Kenny, J. M. (2014). Physical,  
589 structural and antimicrobial properties of poly vinyl alcohol-chitosan biodegradable  
590 films. *Food Hydrocolloids*, 35, 463–470.

591 Burt, S. (2004). Essential oils: Their antibacterial properties and potential applications in  
592 foods - A review. *International Journal of Food Microbiology*, 94(3), 223–253.

593 Can Baser, K. (2008). Biological and pharmacological activities of carvacrol and  
594 carvacrol bearing essential oils. *Current Pharmaceutical Design*, 14(29), 3106–  
595 3119.

596 Cano, A., Jiménez, A., Cháfer, M., González, C., & Chiralt, A. (2014). Effect of  
597 amylose:amylopectin ratio and rice bran addition on starch films properties.  
598 *Carbohydrate Polymers*, 111, 543–555.

599 Cano, A., Fortunati, E., Cháfer, M., Kenny, J. M., Chiralt, A., & González-Martínez, C.  
600 (2015). Properties and ageing behaviour of pea starch films as affected by blend  
601 with poly(vinyl alcohol). *Food Hydrocolloids*, 48, 84–93.

602 Cano, A. I., Cháfer, M., Chiralt, A., & González-Martínez, C. (2016). Biodegradation  
603 behaviour of starch-PVA films as affected by the incorporation of different  
604 antimicrobials. *Polymer Degradation and Stability*, 132, 11–20.

605 Carneiro-da-Cunha, M. G., Cerqueira, M. A., Souza, B. W. S., Souza, M. P., Teixeira, J.  
606 A., & Vicente, A. A. (2009). Physical properties of edible coatings and films made  
607 with a polysaccharide from *Anacardium occidentale* L. *Journal of Food*  
608 *Engineering*, 95(3), 379–385.

609 Carneiro-da-Cunha, M. G., Cerqueira, M. A., Souza, B. W. S., Carvalho, S., Quintas, M.  
610 A. C., Teixeira, J. A., & Vicente, A. A. (2010). Physical and thermal properties of a  
611 chitosan/alginate nanolayered PET film. *Carbohydrate Polymers*, 82(1), 153–159.

612 Cerqueira, M. A., Lima, Á. M., Teixeira, J. A., Moreira, R. A., & Vicente, A. A. (2009).  
613 Suitability of novel galactomannans as edible coatings for tropical fruits. *Journal of*  
614 *Food Engineering*, 94(3–4), 372–378.

615 Collazo-Bigliardi, S., Ortega-Toro, R., & Chiralt, A. (2018). Properties of micro- and  
616 nano-reinforced biopolymers for food applications. *Polymers for Food Applications*  
617 (T. J. Gutiérrez, ed.).

618 Collazo-Bigliardi, S., Ortega-Toro, R., & Chiralt, A. (2019). Using grafted poly( $\epsilon$ -  
619 caprolactone) for the compatibilization of thermoplastic starch-poly(lactic acid  
620 blends. *Reactive and Functional Polymers*.

621 Debeaufort, F., Martin-Polo, M., & Voilley, A. (1993). Polarity homogeneity and structure  
622 affect water vapor permeability of model edible films. *Journal of Food Science*,  
623 *58*(2), 426–429.

624 DeMerlis, C. C., & Schoneker, D. R. (2003). Review of the oral toxicity of polyvinyl  
625 alcohol (PVA). *Food and Chemical Toxicology*, *41*(3), 319–326.

626 Drobot, M., Persin, Z., Zemljic, L., Mohan, T., Stana-Kleinschek, K., Doliska, A.,  
627 Coseri, S. (2013). Chemical modification and characterization of poly(ethylene  
628 terephthalate) surfaces for collagen immobilization. *Open Chemistry*, *11*(11).

629 Fabra, M. J., Flores-López, M. L., Cerqueira, M. A., de Rodriguez, D. J., Lagaron, J. M.,  
630 & Vicente, A. A. (2016). Layer-by-layer technique to developing functional  
631 nanolaminate films with antifungal activity. *Food and Bioprocess Technology*, *9*(3),  
632 471–480.

633 Farrington, D. W., Lunt, J., Davies, S., & Blackburn, R. S. (2005). 6 - Poly(lactic acid)  
634 fibers. In R. S. B. T.-B. and S. F. Blackburn (Ed.), *Woodhead Publishing Series in*  
635 *Textiles* (pp. 191–220).

636 Gennadios A., Weller C. L, & Gooding C. H. (1994). Measurement errors in water  
637 vapour permeability of highly permeable, hydrophilic edible films. *Journal of Food*  
638 *Engineering*, *21*(4), 395-409.

639 Hejda, F., Solař, P., & Kousal, J. (2010). Surface free energy determination by contact  
640 angle measurements – A comparison of various approaches. (3), 25–30.

641 Retrieved online from:  
642 [https://pdfs.semanticscholar.org/e5a0/e7dc916cf7f0b4a3e24027cf7421d5d5e0.p](https://pdfs.semanticscholar.org/e5a0/e7dc916cf7f0b4a3e24027cf7421d5d5e0.pdf)  
643 [df](https://pdfs.semanticscholar.org/e5a0/e7dc916cf7f0b4a3e24027cf7421d5d5e0.pdf) (September 2019)

644 Hsu J. C.-H., & Guckenberger, A. C. (1985). EP0175451A2. Retrieved from  
645 <https://patents.google.com/patent/EP0175451A2/ru> (September 2019)

646 Hutchings, J. B. (1999). Food and colour appearance. Chapman and Hall food science  
647 book, (2nd edition). Gaithersburg, Maryland: Aspen Publication.

648 Kamimura, J. A., Santos, E. H., Hill, L. E., & Gomes, C. L. (2014). Antimicrobial and  
649 antioxidant activities of carvacrol microencapsulated in hydroxypropyl-beta-  
650 cyclodextrin. *LWT - Food Science and Technology*, 57(2), 701–709.

651 Kwok, D. Y., & Neumann, A. W. (1999). Contact angle measurement and contact angle  
652 interpretation. In *Advances in Colloid and Interface Science* (Vol. 81).

653 Medeiros, B. G. d. S., Pinheiro, A. C., Teixeira, J. A., Vicente, A. A., & Carneiro-da-  
654 Cunha, M. G. (2012). Polysaccharide/protein nanomultilayer coatings: construction,  
655 characterization and evaluation of their effect on “Rocha” pear (*Pyrus communis* L.)  
656 Shelf-Life. *Food and Bioprocess Technology*, 5(6), 2435–2445.

657 Medeiros, B. G. d. S., Souza, M. P., Pinheiro, A. C., Bourbon, A. I., Cerqueira, M. A.,  
658 Vicente, A. A., & Carneiro-da-Cunha, M. G. (2014). Physical characterisation of an  
659 alginate/lysozyme nano-laminate coating and its evaluation on “Coalho” cheese  
660 shelf life. *Food and Bioprocess Technology*, 7(4), 1088–1098.

661 Mascheroni, E., Guillard, V., Gastaldi, E., Gontard, N., & Chalier, P. (2011). Anti-  
662 microbial effectiveness of relative humidity-controlled carvacrol release from wheat  
663 gluten/montmorillonite coated papers. *Food Control*, 22(10), 1582–1591.

664 Muller, J., Jiménez, A., González-Martínez, C., & Chiralt, A. (2016). Influence of  
665 plasticizers on thermal properties and crystallization behaviour of poly(lactic acid)  
666 films obtained by compression moulding. *Polymer International*, 65(8), 970–978.

667 Muller, J., González-Martínez, C., & Chiralt, A. (2017a). Poly(lactic) acid (PLA) and  
668 starch bilayer films, containing cinnamaldehyde, obtained by compression  
669 moulding. *European Polymer Journal*, 95(July), 56–70.

670 Muller, J., Casado Quesada, A., González-Martínez, C., & Chiralt, A. (2017b).  
671 Antimicrobial properties and release of cinnamaldehyde in bilayer films based on  
672 polylactic acid (PLA) and starch. *European Polymer Journal*, 96(May), 316–325.

673 Noel, S., Liberelle, B., Yogi, A., Moreno, M. J., Bureau, M. N., Robitaille, L., & De  
674 Crescenzo, G. (2013). A non-damaging chemical amination protocol for  
675 poly(ethylene terephthalate) – application to the design of functionalized compliant  
676 vascular grafts. *J. Mater. Chem. B*, 1(2), 230–238.

677 Ortega-Toro, R., Contreras, J., Talens, P., & Chiralt, A. (2015). Physical and structural  
678 properties and thermal behaviour of starch-poly( $\epsilon$ -caprolactone) blend films for food  
679 packaging. *Food Packaging and Shelf Life*, 5, 10–20.

680 Owusu Apenten, R. K., & Zhu, Q.-H. (1996). Interfacial parameters for selected Spans  
681 and Tweens at the hydrocarbon—water interface. *Food Hydrocolloids*, 10(1), 27–  
682 30.

683 Perdonés, Á., Chiralt, A., & Vargas, M. (2016). Properties of film-forming dispersions  
684 and films based on chitosan containing basil or thyme essential oil. *Food*  
685 *Hydrocolloids*, 57, 271–279.

686 Petersen, K., Væggemose Nielsen, P., Bertelsen, G., Lawther, M., Olsen, M. B.,  
687 Nilsson, N. H., & Mortensen, G. (1999). Potential of biobased materials for food  
688 packaging. *Trends in Food Science and Technology*, 10(2), 52–68.

689 Pinheiro, A. C., Bourbon, A. I., Quintas, M. A. C., Coimbra, M. A., & Vicente, A. A.  
690 (2012). K -carrageenan / chitosan nanolayered coating for controlled release of a  
691 model bioactive compound. *Innovative Food Science and Emerging Technologies*,  
692 16, 227–232.

693 Ramos, M., Beltrán, A., Peltzer, M., Valente, A. J. M., & Garrigós, M. del C. (2014).  
694 Release and antioxidant activity of carvacrol and thymol from polypropylene active  
695 packaging films. *LWT - Food Science and Technology*, 58(2), 470–477.

696 Requena, R., Vargas, M., & Chiralt, A. (2018). Obtaining antimicrobial bilayer starch and  
697 polyester-blend films with carvacrol. *Food Hydrocolloids*, 83, 118–133.

698 Rhim, J. W., Mohanty, K. A., Singh, S. P., & Ng, P. K. W. (2006). Preparation and  
699 properties of biodegradable multilayer films based on soy protein isolate and  
700 poly(lactide). *Industrial and Engineering Chemistry Research*, 45(9), 3059–3066.

701 Ribeiro, C., Vicente, A. A., Teixeira, J. A., & Miranda, C. (2007). Optimization of edible  
702 coating composition to retard strawberry fruit senescence. *Postharvest Biology and  
703 Technology*, 44(1), 63–70.

704 Sapper, M., & Chiralt, A. (2018). Starch-based coatings for preservation of fruits and  
705 vegetables. *Coatings*, 8(5).

706 Sapper, M., Bonet, M., & Chiralt, A. (2019). Wettability of starch-gellan coatings on  
707 fruits, as affected by the incorporation of essential oil and/or surfactants. *Lwt*,  
708 116(March), 108574.

709 Siracusa, V. (2012). Food packaging permeability behaviour: A Report. *International  
710 Journal of Polymer Science*, 2012(i), 1–11.

711 Souza, M. P., Vaz, A. F. M., Costa, T. B., Cerqueira, M. A., De Castro, C. M. M. B.,  
712 Vicente, A. A., & Carneiro-da-Cunha, M. G. (2018). Construction of a biocompatible  
713 and antioxidant multilayer coating by layer-by-layer assembly of  $\kappa$ -carrageenan and  
714 quercetin nanoparticles. *Food and Bioprocess Technology*, 11(5), 1050–1060.

715 Tampau, A., González-Martínez, C., & Chiralt, A. (2018). Release kinetics and  
716 antimicrobial properties of carvacrol encapsulated in electrospun poly-( $\epsilon$ -  
717 caprolactone) nanofibres. Application in starch multilayer films. *Food Hydrocolloids*,  
718 79, 158–169.

719 Tampau, A., González-Martínez, C., & Chiralt, A. (2020). Polyvinyl alcohol-based  
720 materials encapsulating carvacrol obtained by solvent casting and electrospinning.  
721 *Reactive and Functional Polymers*, 153(April), 104603.

722 Turek, C., & Stintzing, F. C. (2013). Stability of essential oils: A Review. *Comprehensive*  
723 *reviews in food science and food safety*, 12(1), 40–53.

724 Xiao, L., Wang, B., Yang, G., & Gauthier, M. (2012). Poly(lactic acid)-based  
725 biomaterials: synthesis, modification and applications. In *Biomedical Science,*  
726 *Engineering and Technology*.

727 Zhu, Y., Gao, C., Liu, X., & Shen, J. (2002). Surface modification of polycaprolactone  
728 membrane via aminolysis and biomacromolecule immobilization for promoting  
729 cytocompatibility of human endothelial cells. *Biomacromolecules*, 3(6), 1312–1319.

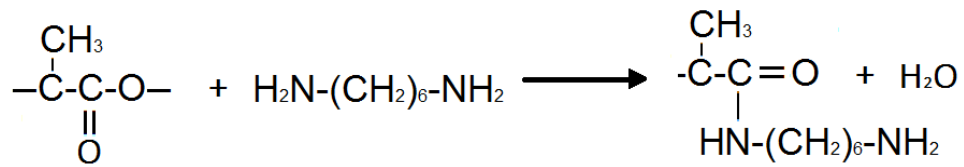
730 Zhu, Y., Gao, C., Liu, X., He, T., & Shen, J. (2004). Immobilization of  
731 biomacromolecules onto aminolyzed poly(L-lactic acid) toward acceleration of  
732 endothelium regeneration. *Tissue Engineering*, 10(1–2), 53–61.

733 [www.accudynetest.com/surface\\_tension\\_table.html](http://www.accudynetest.com/surface_tension_table.html) (page accessed in October 2018)

734 [www.natureworksllc.com/What-is-Ingeo/How-Ingeo-is-Made](http://www.natureworksllc.com/What-is-Ingeo/How-Ingeo-is-Made) (page accessed in May  
735 2019)

736 <http://polymerdatabase.com/Films/Multilayer%20Films.html> (page accessed in October  
737 2019)

738

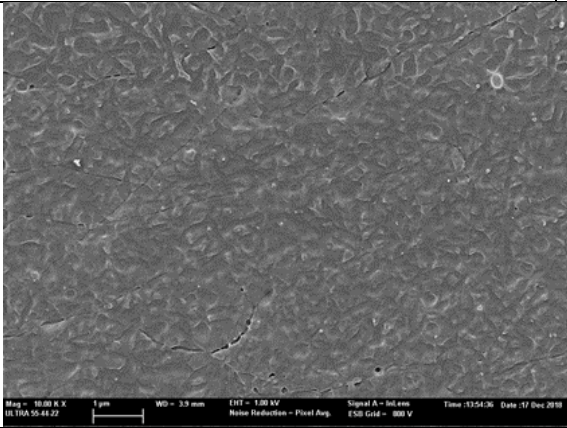
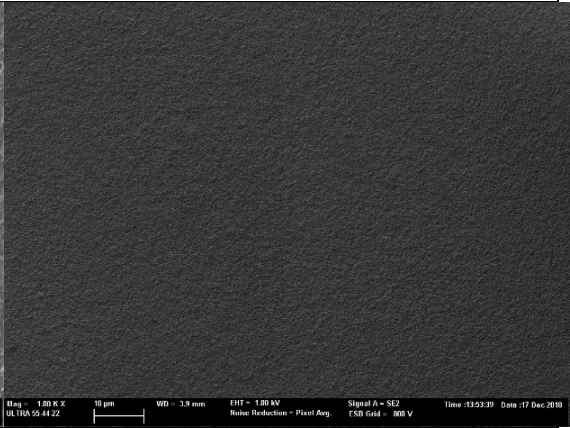
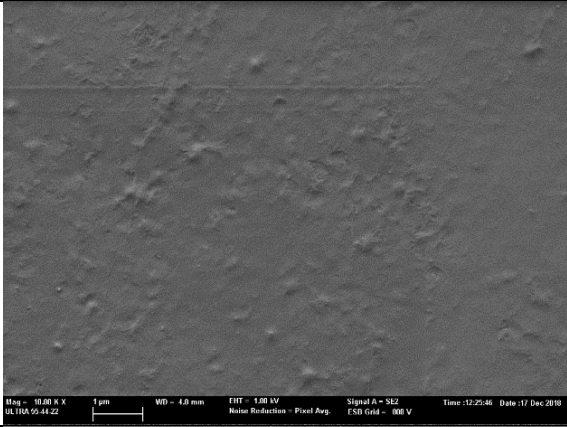
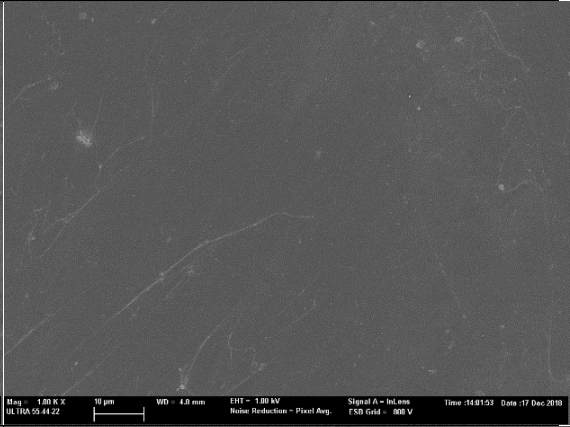
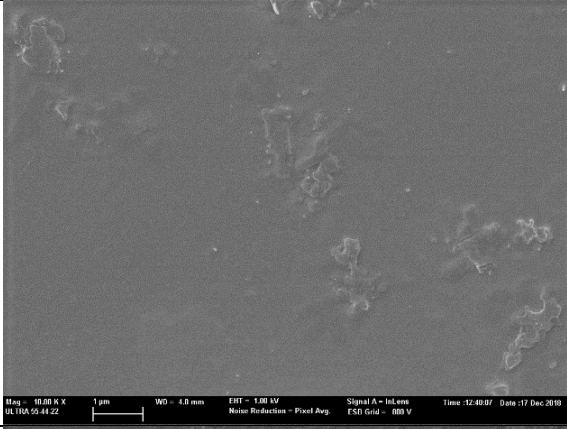
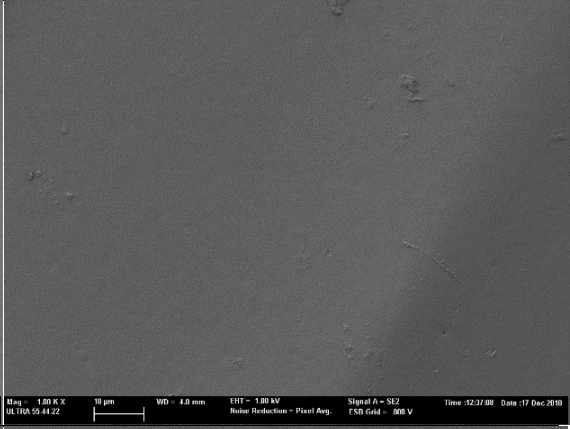
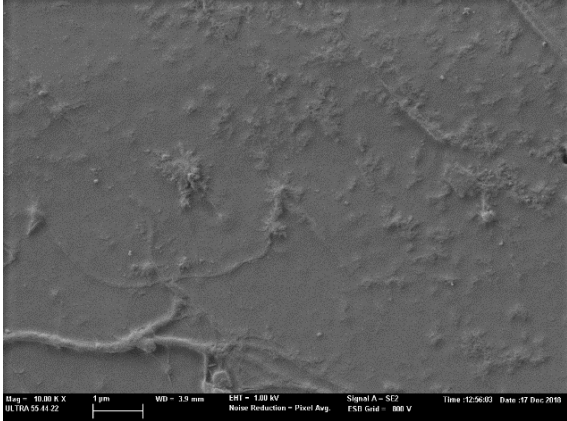
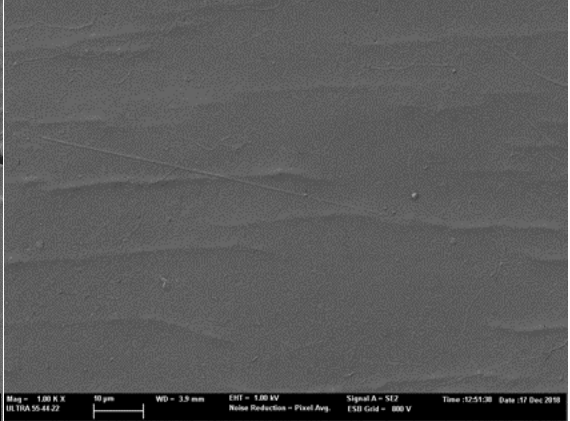


739

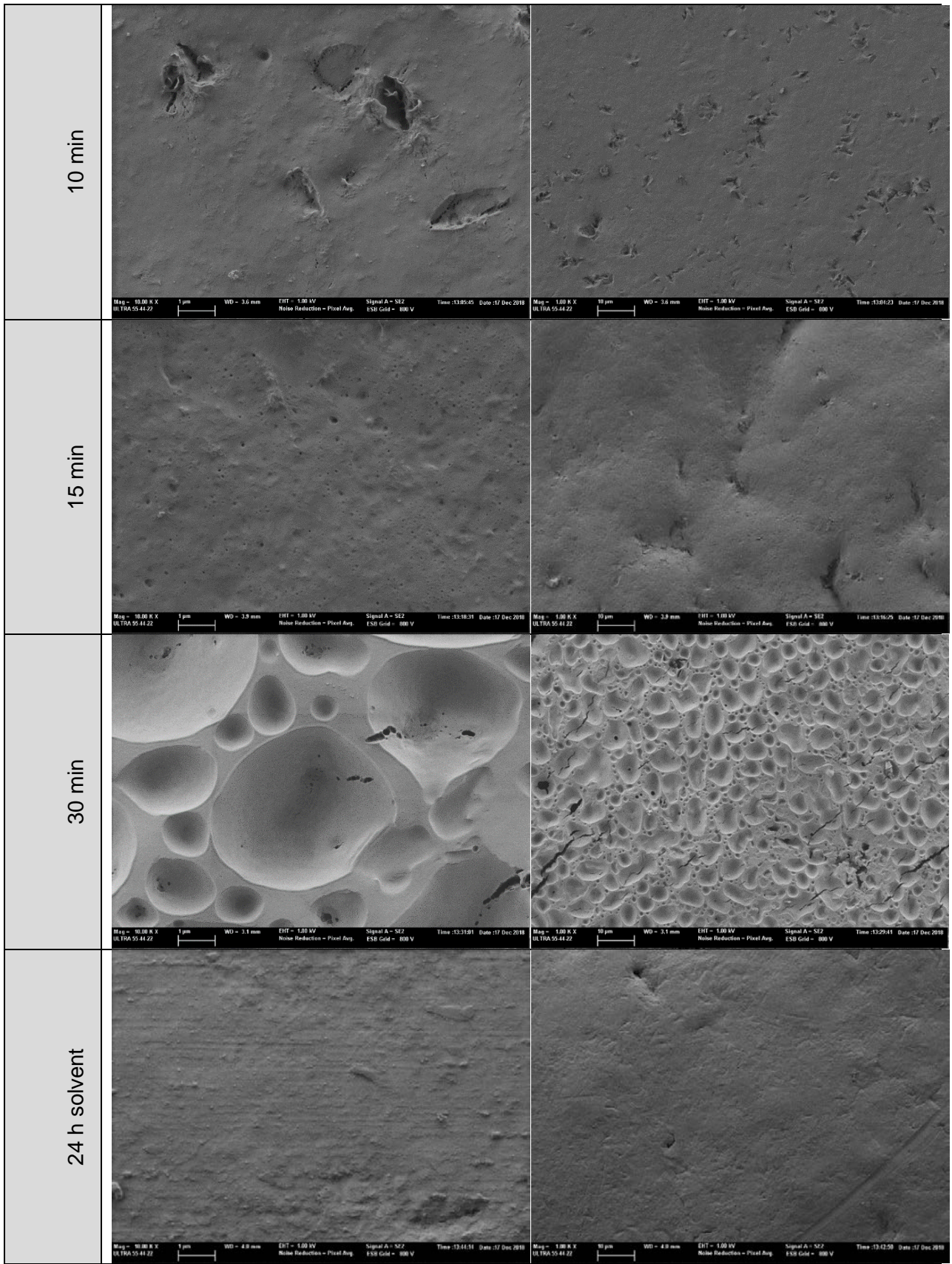
740 **Figure 1.** Mechanism of aminolization by 1,6-hexanediamine, occurring at the

741 polylactide's surface.

742

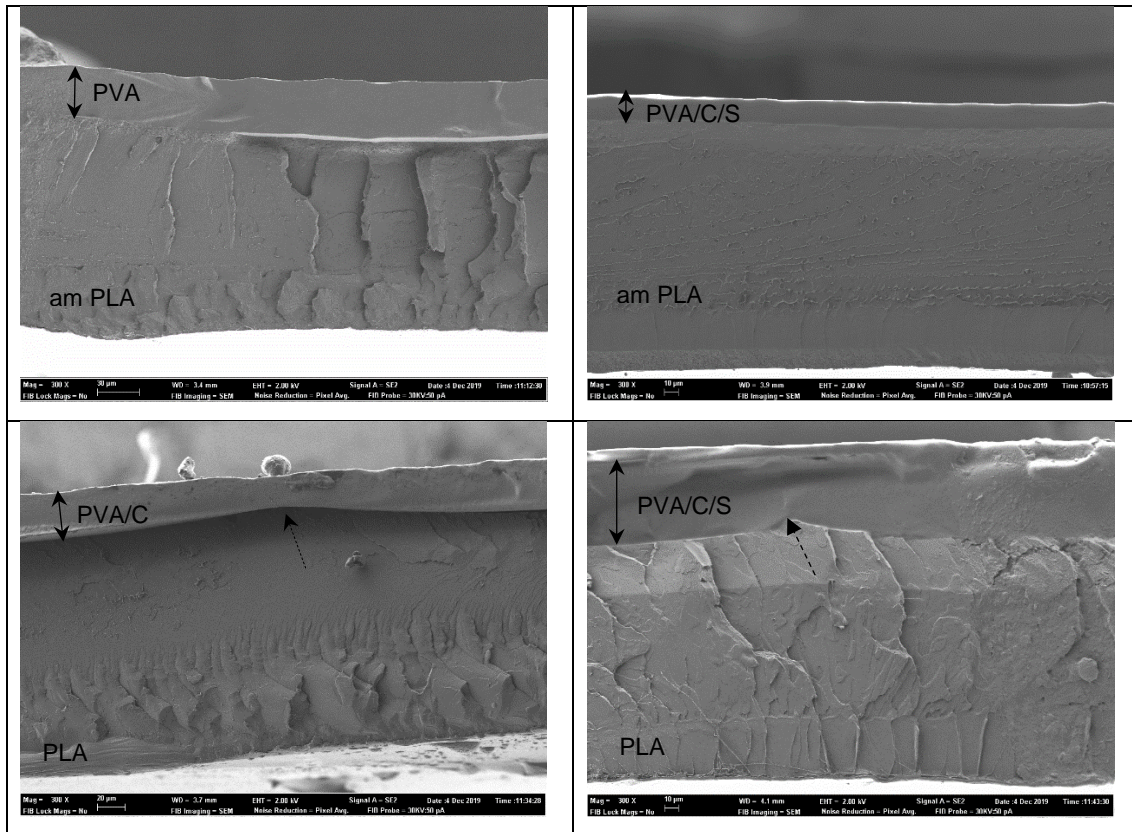
treatment time	Magnification factor	
	x 10 000	x 1000
0 min	 <p>Mag = 10.00 K X ULTRA 55 44 22 1 μm WD = 3.9 mm EHT = 1.00 kV Noise Reduction - Pixel Avg. Signal A - InLens ESB Grid - 000 V Time: 13:54:36 Date: 17 Dec 2019</p>	 <p>Mag = 1.00 K X ULTRA 55 44 22 10 μm WD = 3.9 mm EHT = 1.00 kV Noise Reduction - Pixel Avg. Signal A - SE2 ESB Grid - 000 V Time: 13:53:39 Date: 17 Dec 2019</p>
1 min	 <p>Mag = 10.00 K X ULTRA 55 44 22 1 μm WD = 4.0 mm EHT = 1.00 kV Noise Reduction - Pixel Avg. Signal A - SE2 ESB Grid - 000 V Time: 12:25:46 Date: 17 Dec 2019</p>	 <p>Mag = 1.00 K X ULTRA 55 44 22 10 μm WD = 4.0 mm EHT = 1.00 kV Noise Reduction - Pixel Avg. Signal A - InLens ESB Grid - 000 V Time: 14:01:53 Date: 17 Dec 2019</p>
3 min	 <p>Mag = 10.00 K X ULTRA 55 44 22 1 μm WD = 4.0 mm EHT = 1.00 kV Noise Reduction - Pixel Avg. Signal A - InLens ESB Grid - 000 V Time: 12:40:07 Date: 17 Dec 2019</p>	 <p>Mag = 1.00 K X ULTRA 55 44 22 10 μm WD = 4.0 mm EHT = 1.00 kV Noise Reduction - Pixel Avg. Signal A - SE2 ESB Grid - 000 V Time: 12:37:08 Date: 17 Dec 2019</p>
5 min	 <p>Mag = 10.00 K X ULTRA 55 44 22 1 μm WD = 3.9 mm EHT = 1.00 kV Noise Reduction - Pixel Avg. Signal A - SE2 ESB Grid - 000 V Time: 12:56:03 Date: 17 Dec 2019</p>	 <p>Mag = 1.00 K X ULTRA 55 44 22 10 μm WD = 3.9 mm EHT = 1.00 kV Noise Reduction - Pixel Avg. Signal A - SE2 ESB Grid - 000 V Time: 12:51:38 Date: 17 Dec 2019</p>



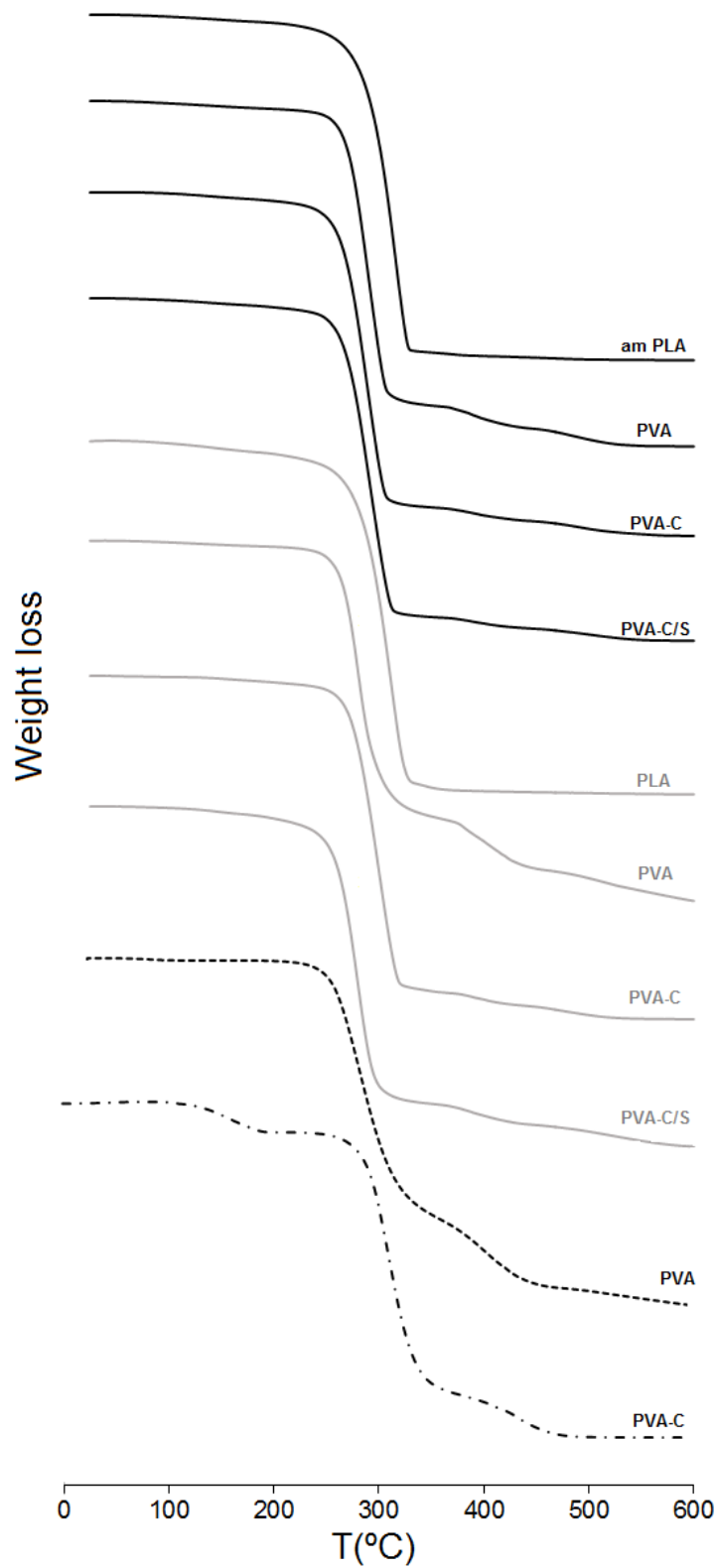


743 **Figure 2.** FESEM micrographs of the PLA film surface submitted to the aminolization  
 744 treatment (different times). Magnification of 10 000 x and 1000 x.

745



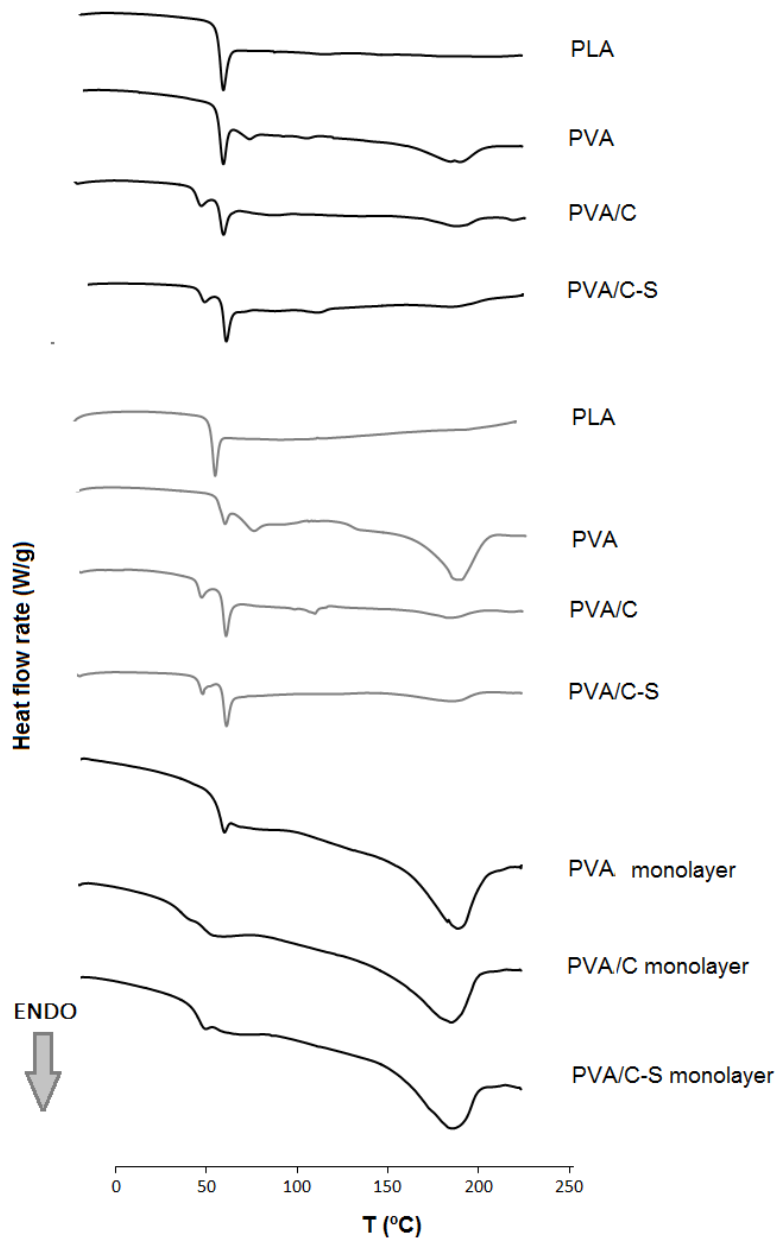
747 **Figure 3.** Micrographs of several bilayer cross-sections. Top row: aminolized PLA with  
 748 PVA (left) and PVA/C/S (right) coatings. Bottom row: untreated PLA with PVA/C (left)  
 749 and PVA/C/S (right) coatings. Dotted arrows indicate protuberances at PLA surface.



751

752 **Figure 4.** TGA curves of multilayer assemblies with PLA, aminolized (black curves) or  
 753 not (grey curves), and PVA, containing or not carvacrol (C) and surfactant (S).

754



755

756 **Figure 5.** DSC curves of multilayer assemblies with PLA, aminolized (black curves) or  
 757 not (grey curves), and PVA, containing or not carvacrol (C) and surfactant (S).  
 758 Monolayers of aminolized PLA (solid black curve), untreated PLA (solid grey curve) and  
 759 PVA also included.

760

761 **Table 1.** Surface energy (SE) and its polar and dispersive components of PLA films  
 762 submitted to different aminolization times. Relative change (%) with respect to the initial  
 763 value in mass ( $\Delta m$ ) and thickness ( $\Delta e$ ) provoked by the process are shown. In brackets,  
 764 the values of mass gain of films immersed only in solvent.

Aminolization time (min)	PLA surface free energy (mN/m)			$\Delta m$ (%)	$\Delta e$ (%)
	SE	Polar component	Dispersive component		
0	29.3	8.8	20.5	n/a	n/a
1	37.0	18.5	18.5	0.5±0.2 (1.2)	7.6
3	37.4	17.6	19.8	0.7±0.2 (5.9)	8.8
5	31.7	9.1	22.6	1.1±0.2 (7.9)	17.2
10	32.3	13.5	18.8	3.2±0.6 (8.4)	21.2
15	n/a	n/a	n/a	4.2±1.2 (7.1)	35.6
30	n/a	n/a	n/a	-5.49 (8.6)	419.2

765

766

767 **Table 2.** Surface tension ( $\gamma_L$ ) of the PVA solutions (C/S wt. ratios are specified) and  
 768 contact angles ( $\theta$ ) on PLA layer as a function of the aminolization time. Different  
 769 superscript letters (a, b, c) and numbers (1, 2, 3) in the same column, and row respectively,  
 770 indicate significant ( $p < 0.05$ ) differences between samples for the analysed parameter.

	<b>PVA</b>	<b>PVA/C</b>	<b>PVA-C/S</b> (0.3:100)	<b>PVA-C/S</b> (0.4:100)	<b>PVA- C/S</b> (0.5:100)
<b><math>\gamma_L</math> (mN/m)</b>	45.4±0.5 <sup>2</sup>	36.0±0.3 <sup>1</sup>	36.1±0.4 <sup>1</sup>	36.0±0.2 <sup>1</sup>	36.5±0.2 <sup>1</sup>
<b>Aminolization time (min)</b>	<b>Contact angles (<math>\theta</math>)</b>				
<b>0</b>	51±1 <sup>c,4</sup>	44±2 <sup>a,23</sup>	38±2 <sup>a,1</sup>	41±2 <sup>a,2</sup>	44±3 <sup>ab,3</sup>
<b>1</b>	44±3 <sup>b,1</sup>	42±1 <sup>a,1</sup>	45±7 <sup>b,1</sup>	44±7 <sup>ab,1</sup>	46±5 <sup>bc,1</sup>
<b>3</b>	33±3 <sup>a,1</sup>	47±6 <sup>a,3</sup>	49±3 <sup>b,3</sup>	48±4 <sup>b,3</sup>	42±3 <sup>a,2</sup>
	<b>Wettability parameter (<math>W_s</math>)</b>				
<b>0</b>	-17.0±1.0 <sup>a1</sup>	-10.0±1.0 <sup>a23</sup>	-7.5±1.0 <sup>b4</sup>	-9.0±0.7 <sup>b3</sup>	-10.5±1.0 <sup>ab2</sup>
<b>1</b>	-13.0±2.0 <sup>b1</sup>	-9.5±1.0 <sup>a2</sup>	-11.0±3.0 <sup>a12</sup>	-11.0±3.0 <sup>ab12</sup>	-11.0±2.2 <sup>a12</sup>
<b>3</b>	-7.0±2.0 <sup>c3</sup>	-12.0±3.0 <sup>a1</sup>	-12.0±1.3 <sup>a1</sup>	-12.0±2.0 <sup>a1</sup>	-9.4±1.2 <sup>b2</sup>

771

772

773 **Table 3.** Barrier and mechanical properties of bilayer PVA-PLA films. Film thickness and transparency (T<sub>i</sub>) are also shown. Different superscript  
 774 letters in the same column indicate significant differences (p<0.05) between samples.

Multilayer components		WVP x 10 <sup>10</sup> (g/Pa·s·m)	OP x 10 <sup>12</sup> (cm <sup>3</sup> /m·s·Pa)	Young Modulus (MPa)	Tensile Strength (MPa)	ε (%)	Thickness (mm)	T <sub>i</sub> at 460 nm (%)
am PLA	PVA	0.28±0.03 <sup>a</sup>	4.45±0.47 <sup>b</sup>	1300±200 <sup>bc</sup>	53±8 <sup>b</sup>	4.9±0.5 <sup>a</sup>	0.251±0.060 <sup>a</sup>	56±13 <sup>a</sup>
	PVA-C	0.36±0.05 <sup>ab</sup>	5.02±0.32 <sup>bc</sup>	1140±150 <sup>ab</sup>	40±7 <sup>a</sup>	5.4±0.4 <sup>ab</sup>	0.231±0.019 <sup>a</sup>	69±10 <sup>b</sup>
	PVA-C/S	0.40±0.09 <sup>b</sup>	5.89±1.07 <sup>c</sup>	1100±300 <sup>a</sup>	41±5 <sup>a</sup>	6.7±2.5 <sup>bc</sup>	0.236±0.013 <sup>a</sup>	60±5 <sup>a</sup>
PLA	PVA	0.37±0.05 <sup>ab</sup>	4.07±0.16 <sup>b</sup>	1400±50 <sup>c</sup>	49±3 <sup>b</sup>	5.8±0.9 <sup>ab</sup>	0.230±0.018 <sup>a</sup>	86.2±0.3 <sup>c</sup>
	PVA-C	0.33±0.01 <sup>ab</sup>	0.15±0.02 <sup>a</sup>	1100±120 <sup>ab</sup>	42±5 <sup>a</sup>	7.9±2.1 <sup>cd</sup>	0.247±0.022 <sup>a</sup>	86±1 <sup>c</sup>
	PVA-C/S	0.36±0.02 <sup>ab</sup>	0.20±0.06 <sup>a</sup>	1150±110 <sup>ab</sup>	41±4 <sup>a</sup>	8.9±1.0 <sup>d</sup>	0.240±0.010 <sup>a</sup>	85±4 <sup>c</sup>
<b>Monolayers</b>								
	PVA	8.05±0.06	0.0015±0.02	54±5	46±6	97±6	0.065±0.002	86±1
	PLA	0.44±0.03	4.66±0.03	1370±34	53±2	4.3±0.2	0.22±0.01	87.7±0.2

775

776

777 **Table 4.** Thermal parameters of polymers in the multilayer assemblies. Values of pure, non-treated polymers are also included. Different  
 778 superscript letters in the same column indicate significant differences ( $p < 0.05$ ) between specimens.

Bilayer/ monolayer		TGA*				DSC				
						1 <sup>st</sup> heating			2 <sup>nd</sup> heating	
		T <sub>onset 1</sub> (°C)	T <sub>peak 1</sub> (°C)	T <sub>peak 2</sub> (°C)	T <sub>peak 3</sub> (°C)	T <sub>g</sub> PLA (°C)	T <sub>g</sub> PVA (°C)	T <sub>peak</sub> (°C)	ΔH (J/g PVA)	T <sub>g</sub> (°C)
am PLA	PVA	248±2 <sup>cd</sup>	286±3 <sup>ab</sup>	392±2 <sup>ab</sup>	511±27 <sup>a</sup>	56±1 <sup>b</sup>	68.4±1.0 <sup>d</sup>	185±1 <sup>ab</sup>	34±4 <sup>a</sup>	52±3 <sup>c</sup>
	PVA-C	244.9±0.3 <sup>bcd</sup>	286±1 <sup>ab</sup>	391±1 <sup>a</sup>	496±6 <sup>a</sup>	56.2±0.4 <sup>b</sup>	43.8±0.3 <sup>a</sup>	187±1 <sup>b</sup>	17±2 <sup>a</sup>	44±1 <sup>a</sup>
	PVA-C/S	246±1 <sup>bcd</sup>	289±1 <sup>b</sup>	393±0 <sup>ab</sup>	508±1 <sup>a</sup>	57.6±0.0 <sup>c</sup>	45.2±0.2 <sup>b</sup>	188±1 <sup>b</sup>	33±28 <sup>a</sup>	49±2 <sup>bc</sup>
PLA	PVA	244±1 <sup>bc</sup>	280±1 <sup>a</sup>	398±2 <sup>b</sup>	508±2 <sup>a</sup>	56.0±1.0 <sup>b</sup>	68.9±0.1 <sup>d</sup>	189±2 <sup>b</sup>	84±43 <sup>b</sup>	53±2 <sup>c</sup>
	PVA-C	251±4 <sup>d</sup>	292±7 <sup>b</sup>	396±1 <sup>ab</sup>	504±28 <sup>a</sup>	57.8±0.7 <sup>c</sup>	44.3±0.7 <sup>ab</sup>	183±1 <sup>a</sup>	25±7 <sup>a</sup>	47±2 <sup>ab</sup>
	PVA-C/S	241±2 <sup>b</sup>	279±2 <sup>a</sup>	392±1 <sup>ab</sup>	530±12 <sup>a</sup>	58.2±0.0 <sup>c</sup>	44.6±0.3 <sup>ab</sup>	186±1 <sup>ab</sup>	23±8 <sup>a</sup>	45±1 <sup>ab</sup>
am PLA		268±1 <sup>e</sup>	310±1 <sup>c</sup>	-	-	55±1 <sup>ab</sup>	-	-	-	51.9±0.1 <sup>c</sup>
PLA		269±5 <sup>e</sup>	310±4 <sup>c</sup>	-	-	54.4±0.2 <sup>a</sup>	-	-	-	53±2 <sup>c</sup>
PVA		192±1 <sup>a</sup>	288±4 <sup>b</sup>	398±6 <sup>b</sup>	-	-	55.0±0.3 <sup>c</sup>	-	50±3 <sup>ab</sup>	63±3 <sup>d</sup>

779 \* no residue was observed at 600 °C.